Continuous in vitro exposure of intestinal epithelial cells to E171 food additive causes oxidative stress, inducing oxidation of DNA bases but no endoplasmic reticulum stress

Marie Dorier, David Béal, Caroline Marie-Desvergne, Muriel Dubosson, Frédérick Barreau, Eric Houdeau, Nathalie Herlin-Boime, Marie Carrière

Continuous in vitro exposure of intestinal epithelial cells to E171 food additive causes oxidative stress, inducing oxidation of DNA bases but no endoplasmic reticulum stress

Marie Dorier[1,2], David Béal[1,2], Caroline Marie-Desvergne[3], Muriel Dubosson[3], Frédérick Barreau[4], Eric Houdeau[5,6], Nathalie Herlin-Boime[7], Marie Carriere[1,2,*]

[1]Univ. Grenoble Alpes, INAC, SyMMES, Chimie Interface Biologie pour l'Environnement, la Santé et la Toxicologie (CIBEST), F-38000 Grenoble, France. marie.dorier@cea.fr; david.beal@cea.fr; marie.carriere@cea.fr; +33438780328.

[2]CEA, INAC, LCIB, Chimie Interface Biologie pour l'Environnement, la Santé et la Toxicologie (CIBEST), F-38054 Grenoble, France,

[3]Univ. Grenoble Alpes, CEA, Nanosafety Platform, Medical Biology Laboratory (LBM), 17 rue des Martyrs, F-38054 Grenoble, France.

[4]INSERM, UMR 1220, Institut de Recherche en Santé Digestive, Toulouse, France. frederick.barreau@inserm.fr; +33562744504.

[4]INRA, UMR1331 Toxalim, Research Center in Food Toxicology, F-31027 Toulouse, France. eric.houdeau@inra.fr; +33582066300.

[5]Université de Toulouse, UPS, UMR1331, Toxalim, F-31062 Toulouse, France.

[6]NIMBE, CEA, CNRS, Université Paris-Saclay, CEA Saclay 91191 Gif-sur-Yvette France. nathalie.herlin@cea.fr; +33169083684.

*Corresponding author: Dr. Marie Carriere. E-mail: marie.carriere@cea.fr; Phone +33 4 38 78 03 28; Fax: +33 4 38 78 50 90; ORCiD : 0000-0001-8446-6462.

Abstract

The whitening and opacifying properties of titanium dioxide are commonly exploited when it is used as a food additive (E171). However, the safety of this additive can be questioned as TiO_2 nanoparticles (TiO_2-NPs) have been classed at potentially toxic.

This study aimed to shed some light on the mechanisms behind the potential toxicity of E171 on epithelial intestinal cells, using two in vitro models: i) a monoculture of differentiated Caco-2 cells, and ii) a coculture of Caco-2 with HT29-MTX mucus-secreting cells. Cells were exposed to E171 and two different types of TiO_2-NPs, either acutely (6 to 48 h) or repeatedly (twice a week for 3 weeks).

Our results confirm that E171 damaged these cells, and that the main mechanism of toxicity was oxidation effects. Responses of the two models to E171 were similar, with a moderate, but significant, accumulation of reactive oxygen species, and concomitant downregulation of the expression of the antioxidant enzymes catalase, superoxide dismutase and glutathione reductase. Oxidative damage to DNA was detected in exposed cells, proving that E171 effectively induces oxidative stress; however, no endoplasmic reticulum stress was detected. E171 effects were less intense after acute exposure compared to repeated exposure, which correlated with higher Ti accumulation. The effects were also more intense in cells exposed to E171 than in cells exposed to TiO_2-NPs.

Taken together, these data show that E171 induces only moderate toxicity in epithelial intestinal cells, via oxidation.

Keywords

TiO_2, E171, intestine, toxicity, endoplasmic reticulum stress

Introduction

Titanium dioxide (TiO_2) has been used as a white pigment and opacifying agent for many years. Its many applications include as an additive in paints, plastics, paper, and food. As a food additive, the European nomenclature refers to TiO_2 as E171, and its use has been authorized since 1969 thanks to evidence indicating low intestinal absorption, solubility and toxicity (Amenta, 2015; Jovanovic, 2015). The characteristics of E171 were reevaluated in 2016 by the European Food Safety Authority (EFSA), which concluded on extremely low absorption of orally-administered TiO_2, regardless of particle size (EFSA, 2016). Based on the existing literature at that time, no acceptable daily intake value could be defined. According to the European recommendations defining nanomaterials (2011/696/EU), E171 is not a nanomaterial. However, it can contain up to 43% of TiO_2-NPs (Chen, 2013; Peters, 2014; Weir, 2012; Yang, 2014), and these nanoparticles may have toxic effects (Grande, 2016; McCracken, 2016; Shi, 2013). E171 is used in a wide range of food products, in particular confectionery and chewing gums (Peters, 2014; Weir, 2012), with between 0.02 and 9.0 mg/g TiO_2 found in some food and personal care products, of which 5-10% corresponds to TiO_2-NPs (Peters, 2014). Based on these data, human daily exposure through ingestion was initially estimated to range between 0.035 mg/kg of body weight (b.w.)/day (Frohlich, 2012) and 5 mg/person (Powell, 2010), with differences depending on the age of the individual: 1-2 mg TiO_2/kg b.w. for US children under 10 years of age, and 0.2-0.7 mg TiO_2/kg b.w. for other US consumers (Weir, 2012). More recently, these estimations were refined, and exposure was reported to range between 0.2 and 0.4 mg/kg b.w. in infants and the elderly, and 5.5 to 10.4 mg/kg b.w. in children, depending on the exposure scenario (EFSA, 2016). Within the Dutch population, daily exposure has been estimated at 4.2 mg/kg b.w. for children between 2 and 6 years of age, 1.6 mg/ kg b.w. for 7-69 year-old consumers, and 0.74 mg/kg b.w. for older consumers (Rompelberg, 2016). Based on these refined estimations of intake, an extensive

review of the existing literature assessing the risks associated with ingested TiO_2-NPs and toxicokinetic data concluded that a risk for the liver and reproductive organs could not be excluded (Heringa, 2016).

While the impact of inhaled TiO_2 has been extensively studied and reviewed (Johnston, 2009; Shi, 2013; Skocaj, 2011), the oral route has been less well-documented (McCracken, 2016; Skocaj, 2011). When ingested by human volunteers, E171 was found to be absorbed in the gastrointestinal tract at low levels (Pele, 2015). In rats, it impaired intestinal immune homeostasis (Bettini, 2017), and its consumption was linked to colorectal cancer (Bettini, 2017; Urrutia-Ortega, 2016). However, no acute or sub-chronic toxicity was observed in rats ingesting TiO_2 particles with the same size distribution and crystalline structure as E171 (Warheit, 2015), although toxic effects were reported with TiO_2-NPs of different sizes and crystal phases. These effects were observed on the cardiovascular system (Chen, 2015; Wang, 2007; Wang, 2013), the kidneys (Al-Rasheed, 2013; Wang, 2007), the liver (Wang, 2007) or reproductive organs (Jia, 2014).

The mechanisms behind these effects are not well known. Inhaled TiO_2-NPs cause oxidative stress in lung cells which drives inflammation, genotoxicity, cytotoxicity and impairs the autophagic process (Johnston, 2009; Shi, 2013). Ingested TiO_2-NPs may cause oxidative stress, and/or may be associated with damage to DNA and cytotoxicity depending on their crystal structure, their size and the differentiation state of cells (Brun, 2014; Dorier, 2015; Gerloff, 2012; Tay, 2014). TiO_2 extracted from chewing gum was reported to increase levels of reactive oxygen species (ROS) in cells without causing any cytotoxicity to intestinal or gastric cells (Chen, 2013). Pre-treatment of E171 with simulated digestive fluids increased intracellular accumulation and inhibited growth in undifferentiated Caco-2 cells but not differentiated Caco-2 cells (Song, 2015).

The present study aimed to identify the mechanisms behind the intestinal toxicity of E171. The impact of E171 was assessed on two *in vitro* models of the ileum: i) differentiated Caco-2 absorptive cells, and ii) a mucus-secreting model composed of Caco-2 cells (70%) co-cultured with HT29-MTX mucus cells (30%). HT29-MTX cells are adapted from the HT29 cell line, by growth in medium containing methotrexate (MTX) (Lesuffleur, 1990). At post-confluence, these cells are totally differentiated into mucus-secreting cells, with appearance of mucus droplets in the culture and expression of MUC1, MUC2, MUC3, MUC4 and MUC5C glycoprotein and mucins (Lesuffleur, 1993). Mucus secretion is then maintained even after reversion to MTX-free medium. Both cell models were either acutely exposed to E171 for 6 h or 48 h, or repeatedly exposed twice a week during their differentiation (21 days). These exposure regimes were designed to mimic acute exposure - when the food bolus reaches the intestine - or the effects of repetitive consumption of TiO_2 on the continuously renewing intestine. Cells were also exposed to two different TiO_2-NPs, i) mixed anatase/rutile TiO_2-NP, measuring 24 nm in diameter (JRCNM01005a from the European Commission Joint Research Center), which has been widely used in toxicity studies, and ii) A12, a 12-nm pure anatase TiO_2-NP, which had a composition close to that of the E171 tested. Cell viability, cell redox status and DNA integrity were monitored, and endoplasmic reticulum (ER) stress was assessed as it can be triggered by oxidative stress and has been associated with inflammatory bowel diseases (Deuring, 2011). The biological responses observed correlated with intracellular accumulation of Ti.

Material and Methods

Chemicals and reagents

Unless otherwise indicated, all chemicals were purchased from Sigma-Aldrich and were >99% pure. Cell culture medium and fetal bovine serum were purchased from Thermo Fisher Scientific.

Particle dispersion and characterization

E171 food additives were purchased as powders from commercial websites. P25 TiO_2-NP is referenced as JRCNM01005a (previously NM105) in the nanomaterials library at the European Joint Research Center (JRC, Ispra, Italy). A12 was synthesized in our laboratories (Pignon, 2008) and was used in our previous studies (Brun, 2014; Dorier, 2015; Jugan, 2012; Simon-Deckers, 2008). The specific surface area of all TiO_2 forms was measured according to Brunauer, Emmett and Teller (BET), and their crystalline phase was determined by X-ray diffraction. Particle diameters were measured by transmission electron microscopy (TEM). Powders were suspended in ultrapure sterile water (10 mg/mL), then sonicated for dispersion using an indirect cup-type sonicator (Cup Horn; Bioblock Scientific, Vibracell 75041) in continuous sonication mode for 30 min, 4 °C), at 52.8 W (80% amplitude), as determined by calorimetry (Taurozzi, 2011). The zeta potential and agglomeration state of suspensions were monitored using a Malvern NanoZS.

Cell culture and exposure

Caco-2 cells (ATCC HTB-37, passages 49 to 60) and HT29-MTX mucus-secreting cells (passages 21 to 35 after differentiation; kindly provided by T. Lesuffleur, INSERM U843, Paris, France) were grown in Dulbecco's Modified Eagle Medium (DMEM)/GlutaMAX™, 10% heat inactivated fetal bovine serum (FBS), 1% non-essential amino acids, 50 units/ml

penicillin and 50 µg/ml streptomycin, at 37 °C in a humidified 5% CO_2 atmosphere. Cells were grown as a monoculture of Caco-2 or as a coculture composed of 70% Caco-2 and 30% HT29-MTX, which is a model of mucus-secreting absorptive epithelium (Lesuffleur, 1990). Mucus secretion and alkaline phosphatase activity were characterized (Figure S1), as a marker of differentiation of microvilli. The techniques used are fully described in the Supplemental Materials and Methods.

For acute exposure experiments, cells were grown to confluence and culture was continued for 21 days post-confluence to promote differentiation, changing culture medium three times a week. Differentiated cells were exposed for 6 h, 24 h or 48 h to E171 or TiO_2-NPs (1-200 µg/mL) in complete cell culture medium. Cells were then harvested (Figure S2). In the repeated exposure regimen, cells were seeded at day 0; the cell culture medium was replaced three times a week with fresh medium containing 1-100 µg/mL E171 or TiO_2-NPs, from day 1 to day 21 post-seeding. Exposure medium containing particles was thus changed a total of eight times (Figure S2). Cells were not subcultured during this period. As calculated previously (Brun, 2014), the exposure concentrations exceeded the estimated human daily exposure to TiO_2 approximately 10,000-fold. After repeated exposure, cell differentiation status was checked; tight junctions (Figure S3A) and microvilli (Figure S3B) showed typical morphologies and mucus secretion was equivalent in exposed cells vs. control cells (Figure S3C-E).

Quantification of intracellular Ti accumulation

In exposed cells, Ti content was measured by Inductively Coupled Plasma Mass Spectrometry (ICP-MS). After exposure, cells were rinsed four times with PBS to remove particles that may be weakly bound to cell membrane before harvesting in 125 µL of ultrapure water. Cells were lysed by microwave-assisted acid decomposition, as previously described (Dorier, 2015).

Briefly, 6 mL of 24 % (vol./vol.) ultrapure grade H_2S0_4 was added to cellular suspensions, which were then heated for 30 min at 1100 W, samples were then diluted in ultrapure grade HNO_3 (1% vol./vol.) and analyzed on a Nexion 300X ICP-MS (Perkin Elmer) equipped with a concentric nebulizer and operated in standard mode. Calibration curves were obtained using a certified ionic Ti ICP-MS standard. Concentrations of ^{47}Ti, ^{48}Ti and ^{49}Ti were analyzed; but final results were only interpreted based on ^{47}Ti as S content (from H_2SO_4) interfered with ^{48}Ti and ^{49}Ti readings.

Cell viability assessment

In the acute exposure regimen, cytotoxicity was assessed using the WST-1 assay (Roche). Cells were grown in 96-well plates, and exposed to 0-200 µg/mL of particles for 6 h or 48 h. Exposure medium was then replaced by 100 µL of WST-1 diluted to 1:10 (vol.:vol.) in cell culture medium, and plates were incubated for 90 min at 37 °C. To avoid particle interference with the assay, plates were centrifuged for 5 min at 200 × *g*, to settle particles at the bottom of wells. Supernatant (50 µL) was then transferred to a clean plate and absorbance was measured at 438 nm using a SpectraMax M2 spectrophotometer (Molecular Devices). Absorbance was normalized by subtracting absorbance readings for control (untreated) wells. Potential interference was checked for as previously described (Brun, 2014); no interference was detected. In the repeated exposure regimen, cell viability in the Caco-2 monoculture was assessed using the trypan blue exclusion assay. Viable and non-viable cells were counted using an automatic cell counter (Countess automatic cell counter, Invitrogen). Cytotoxicity was assessed for the Caco-2/HT29-MTX coculture model based on propidium iodide (PI) exclusion. Cells were incubated with PI before counting using a FacsCalibur analyzer (BD Biosciences) equipped with CXP software (Beckman Coulter). Mean fluorescence was analyzed using Flowing Software 2.5.1 (http://www.flowingsoftware.com/). In both exclusion

assays, measurements were performed in triplicate for each condition; results are expressed as the mean percentage of viable cells after normalization relative to the untreated control.

Quantification of Reactive Oxygen Species

Intracellular ROS content was quantified using 2',7'–dichlorodihydrofluorescein diacetate acetyl ester (H_2-DCF-DA) (Invitrogen). Cells were grown in 12-well plates and exposed to particles, then washed twice with PBS, incubated for 30 min with 80 µM H_2-DCF-DA at 37 °C, and harvested by scraping. Fluorescence intensity was measured with excitation at 480 nm and emission at 530 nm, on a SpectraMax M2 (Molecular Devices). The emission intensity was normalized for protein concentration, as determined using Bradford reagent. Potential interference of TiO_2 particles was tested by measuring DCF fluorescence, either in cells exposed to particles without H_2-DCF-DA, or in particle suspensions (10, 50 and 100 µg/mL) to which H_2-DCF-DA was added. No interference was detected (Table S1).

Genotoxicity

DNA strand breaks, alkali-labile sites, and formamidopyrimidine DNA glycosylase (Fpg)-sensitive sites were assessed using the alkaline version of the comet assay and its Fpg-modified version (Tice, 2000). Cells were grown in 12-well plates, exposed to particles, then harvested and stored at -80 °C in 85.5 g/L sucrose, 11.76 g/L sodium citrate, 50 mL/L DMSO, pH 7.6. Cells were then embedded in 0.5% low-melting-point agarose and spread on glass slides pre-coated with 1% agarose. After cell lysis by immersion in 2.5 M NaCl, 100 mM EDTA, 10 mM Tris, pH 10, 10% DMSO overnight at 4 °C, slides were rinsed in 0.4 M Tris-HCl pH 7.4. Three slides were incubated with Fpg buffer only and another three slides were incubated with Fpg enzyme prepared in Fpg buffer (0.05 U/µL, Interchim), for 45 min at 37 °C. Slides were cooled on ice, before immersion in cold migration buffer (NaOH 300 mM,

EDTA 1mM) for 30 min to allow DNA to unwind. Electrophoresis was performed at 25 V, 300 mA for 30 min. Slides were neutralized by washing three times in 0.4 M Tris-HCl, pH 7.4, then stained with Gel Red (VWR). %tail DNA was measured on 50 nuclei using Comet IV software (Perceptive instruments). As positive control for comet-Fpg, A549 cells were exposed to 1 µM riboflavin for 20 min at 37 °C and then UVA-irradiated (010.0 J/cm²). As positive control for comet alkaline assay, control (unexposed cells) slides were exposed to 50 mM H_2O_2. Experiments were performed in three independent replicates. Results were normalized for %tail DNA in control (unexposed) cells, and expressed as mean fold-change ± standard error calculated over the three independent experiments.

Gene expression

To assess ER stress, levels of classical ER stress markers was monitored based on mRNA expression. The markers analyzed were *IRE-1*, *PERK* and *ATF6*, which encode ER stress sensors that initiate the unfolded protein response (UPR) signaling cascade; and *GRP78/BiP*, which encodes a chaperone that controls protein quality and activates signaling molecules in the ER. We also monitored mRNA levels for *ATF6* and *XBP1*, which encode proteins mediating the UPR mechanism of action, and *CHOP*, which is involved in ER-stress-induced apoptosis (Chaudhari, 2014; Zhang, 2008). Oxidative stress was assessed based on the mRNA expression of antioxidant enzymes, catalase (*CAT*), superoxide dismutases 1 and 2 (*SOD1*, *SOD2*) and glutathione reductase (*GSR*). Gene expression was assessed by reverse transcription-quantitative PCR (RT-qPCR). mRNA was extracted using GenElute™ mammalian total RNA Miniprep kit (Sigma) and stored at -80 °C. Purity was checked using a spectrophotometer (NanoDrop) to measure absorbance at 260 nm (abs260), and determine abs260/abs280 and abs260/abs230 ratios. mRNA was reverse-transcribed using SuperScript III Reverse Transcriptase (Invitrogen). Total cDNA concentration and purity were

determined. MESA Blue qPCR Mastermix for SYBR Assay (Eurogentec) with ROX reference was used to perform the quantitative PCR in a MX3005P thermocycler (Stratagene). The following thermal cycling steps were applied: 95 °C for 5 min, then 95 °C for 15 s, 55 °C for 20 s and 72 °C for 40 s for 40 cycles. For the dissociation curve: 95 °C for 1 min, 55 °C for 30 s and 95 °C for 30 s. Primer sequences are indicated in Table S2; their efficiency was determined to be between 1.8 and 2.2. Relative expression values were calculated as $2^{-\Delta\Delta Cq}$, where ΔCq is the difference between the cycle threshold (Cq) value for target and reference genes and ΔΔCq the difference between the ΔCq in exposed cells vs. control (unexposed) cells. *CYCLOA*, *CYCLOB*, *S18* and *GAPDH* were used as reference genes. Variability of expression for reference genes was assessed using Bestkeeper (Pfaffl, 2004). Gene expression levels were determined and statistically analyzed using the Relative Expression Software Tool (REST2009) (Pfaffl, 2002).

Statistical analysis

Unless indicated otherwise, statistical significance was assessed by applying two tests: Kruskal-Wallis (non-parametric one-way analysis of variance on ranks) and Mann-Whitney U-test, a paired comparison. Statistical analysis was performed using Statistica 8.0 (Statsoft, Chicago, USA). A p-value < 0.05 was taken as the threshold for statistical significance.

Results

Physico-chemical characterization of the particles making up E171 samples and NPs

Five batches of commercially-available E171 were purchased and characterized (Table S3). The characteristics of all batches were comparable; two batches were pure anatase, whereas the other three batches were mainly anatase with traces of rutile (<1%). The average primary diameter of the particles ranged between 100 and 136 nm, as measured on transmission electron microscopy (TEM) images. The percentage of particles with diameter <100 nm, i.e., NPs, ranged from 30% to 55%, in the number size distribution. We selected E171A for the tests to assess E171 toxicity because it was sold in large quantities. This product was composed of round particles (Figure 1A) with a broad size distribution centered on 119±65 nm (Figure 1B). Particles with diameters <100 nm accounted for 47% of the product (Figure 1B), and X-ray diffraction analysis indicated that it was pure anatase (Figure 1C-D). The specific surface area (SSA) for this product was 9.4 m^2/g. After high-energy sonication in water, a hydrodynamic diameter of 415.4±69.5 nm was determined. This diameter increased to 739.3±355.3 nm after dilution in cell culture medium due to particle agglomeration (Table 1). Polydispersity of the suspension was high, with polydispersity indexes (PdI) of 0.48 in water and 0.64 in exposure medium.

P25 and A12 NPs were previously characterized and used in our laboratory (Brun, 2014; Dorier, 2015; Jugan, 2012; Simon-Deckers, 2008); their main characteristics are summarized in Table 1. A12 was pure anatase with a diameter of 12±3 nm. P25 was mixed anatase/rutile (86 %/14 %) TiO_2-NP, with a mean diameter of 24±6 nm. The hydrodynamic diameter of A12 was 85.0±2.9 nm in water and increased to 447.9±0.3 nm when diluted in cell culture medium. For P25, the hydrodynamic diameter was 157.6±1.0 nm in water and 439.9±6.7 nm in cell culture medium. PdI were low for both NPs, suggesting that the suspensions were homogeneously dispersed and stable.

Intracellular accumulation and/or membrane absorption of Ti

One of the aims of this study was to compare the response of two cell models to three types of particles, therefore we first compared their intracellular accumulation. Ti content was measured by ICP-MS in cells after exposure to 50 µg/mL of A12, P25 or E171, either as acute doses for 6 h or 48 h, or repeatedly for 21 days (Table 2). ICP-MS gives an overall quantification of Ti in lysed cells, but it cannot discriminate between Ti accumulated inside the cell and Ti bound to the cell membrane. Whatever the exposure conditions, Ti accumulation in Caco-2 cells was slightly higher than in Caco-2/HT29-MTX cells, but the difference was not statistically significant. TEM images of Caco-2/HT29-MTX cells exposed for 21 days to E171 are provided in Figure S4, showing agglomerates of E171 accumulated in the cytoplasm, entrapped in a vesicle.

In contrast, there were differences depending on the type of particle. Thus, E171 accumulated more than P25, which accumulated more than A12 (E171>>P25>A12). Accumulation was also influenced by the exposure time, with systematically greater accumulation in repeatedly-exposed cells, compared to acutely-exposed cells. In the Caco-2 cell model, accumulation was also significantly higher after 48 h of exposure compared to 6 h of exposure.

Impact of exposure to TiO_2 particles on cellular viability

Since particles accumulated in cells, they could potentially affect cell viability. We therefore assessed cytotoxicity in cell cultures, following exposure. No effect on cell viability was observed in either cell model in the tested conditions (Figure 2).

Oxidative stress

Oxidative stress is reported to be the main mechanism of toxicity induced by TiO_2-NPs (Johnston, 2009; Shi, 2013). For this reason, the redox balance was evaluated in both cell models after exposure to E171 or TiO_2-NPs.

First, intracellular ROS content was quantified using the H_2-DCF-DA assay. In Caco-2 cells exposed to an acute dose of E171 for 48 h, intracellular ROS content was significantly higher than in untreated cells, at all concentrations tested (Figure 3A). A similar increase was observed in Caco-2/HT29-MTX cells at all three time-points (6 h, 24 h, 48 h, acute exposure), and ROS levels were found to increase in a dose-dependent manner (Figure 3B). Similarly, in both cell models, intracellular ROS levels were higher in repeatedly-exposed cells than in untreated cells (Figure 3C-D). Cells repeatedly exposed to E171 did not display higher ROS levels than acutely-exposed cells. TiO_2-NPs also caused intracellular accumulation of ROS, although to a lesser extent than E171.

To confirm that exposure to E171 and TiO_2-NPs induced oxidative stress, the expression of genes encoding antioxidant enzymes – catalase (*CAT*), glutathione reductase (*GSR*), and superoxide dismutases 1 and 2 (*SOD1, SOD2*) – was measured by RT-qPCR. In general, modulation of gene expression was not significantly different in acutely-exposed Caco-2 and Caco-2/HT29-MTX cells, although in Caco-2/HT29-MTX exposed for 48 h to A12 a difference was noted (Table S4). In repeatedly-exposed cells, gene expression was unchanged in the Caco-2 monoculture (Figure 4A), whereas in repeatedly-exposed Caco-2/HT29-MTX, *CAT* and *GSR* were downregulated upon exposure to 10 µg/mL E171, and *GSR* and *SOD1* were downregulated in response to 50 µg/mL E171 (Figure 4B). Exposure to 10 µg/mL A12 caused *CAT* and *SOD1* downregulation; P25 only induced downregulation of *SOD1* (Table S4). Finally, the mRNA expression level for *NRF2* - a transcription factor controlling the

expression of some of these antioxidant enzymes - was measured; no significant change was observed in any of the exposure conditions tested (Table S4).

Oxidative damage to DNA

Oxidative stress can cause oxidative damage to DNA, which can be quantified using the comet assay in its alkaline and Fpg-modified versions. These assays probe DNA strand breaks and alkali-labile sites (alkaline version of the assay) and Fpg-sensitive sites including the 8-oxo-dGuo oxidized base (Fpg-modified version of the assay). In cells exposed to E171 in the acute exposure scenario, no significant DNA damage was observed (Table S5). In contrast, in repeatedly-exposed cells, a significant increase in %tail DNA was observed, in the Fpg-modified version of the comet assay only, in Caco-2 cells exposed to 10 or 50 µg/mL E171, and in Caco-2/HT29-MTX cells exposed to 50 µg/mL E171 (Table 3). Exposure to TiO_2-NPs did not cause oxidative damage to DNA in our assays (Table 3, Table S5).

Endoplasmic reticulum stress

ER homeostasis is strictly controlled by the cellular redox status (Malhotra, 2007). ER stress is classically assessed based on expression levels of markers of the UPR. The mRNA expression of five of these markers, which are typically up-regulated in ER stress conditions, was measured in cells exposed to E171 and TiO_2-NPs to assess ER homeostasis. Unexpectedly, acute exposure to E171 for 48 h induced a significant decrease in the expression of *ATF6* in Caco-2 cells (Figure 5A). Similarly, in Caco-2/HT29-MTX cells, *CHOP*, *ATF6*, *GRP78* and *IRE-1* were downregulated after exposure to E171 (Figure 5B). Repeated exposure of Caco-2 cells to E171 induced downregulation of *CHOP* and *GRP78* (Figure 5C), whereas in Caco-2/HT29-MTX cells it led to downregulation of *sXBP1* (Figure 5D).

Some of these markers were also downregulated in cells exposed to TiO_2-NPs. Thus, in Caco-2 cells exposed to A12, whatever the conditions, and in Caco-2/HT29-MTX repeatedly exposed to P25, *CHOP* expression was decreased. In both cell models repeatedly exposed to P25, *GRP78* was decreased, and in Caco-2 cells repeatedly exposed to P25, *ATF6* levels were lower than in control cells (Table S6).

Discussion

The objective of the present study was to shed some light on the mechanisms behind the potential toxicity of E171 on intestinal cells. Two *in vitro* models of the human ileum were used, the first one was a culture of enterocytes alone, while the second one consisted of enterocytes and mucus-secreting cells. Both models were exposed to E171 or two types of TiO_2-NPs in two different exposure regimes: acute (6 h to 48 h), or repeated (three times a week for 3 weeks) as a simulation of chronic exposure that would result from daily consumption of food containing this additive. The cellular responses to this exposure were monitored.

In terms of toxicological impact of E171, the results of this study indicate that: i) E171 is only moderately toxic to the two cell models tested; ii) repeated exposure triggers an increased cellular response compared to acute exposure; iii) cells respond more to E171 than to TiO_2-NPs, iv) the two cell models respond similarly to E171; and v) the main mechanism driving the toxicity of E171 is oxidative stress.

The exposure conditions used were harsh, with high concentrations and long exposure times. But nevertheless, the overall impact of E171 was modest. The only responsive endpoint identified was oxidative stress, including moderate intracellular accumulation of ROS and

downregulation of expression levels for antioxidant enzymes. That the level of oxidative stress induced was damaging was confirmed by the increase in the level of Fpg-sensitive DNA lesions observed, primarily 8-oxo-dGuo. These lesions are considered mutagenic, because 8-oxo-dGuo can pair with adenine and cytosine with equal efficiency (Carriere, 2017). Therefore, the accumulation of 8-oxo-dGuo observed in this study could cause the cell transformation reported by others upon chronic *in vitro* exposure of lung cells to TiO_2-NPs (Vales, 2015). Our results thus indicate that the main mechanism behind E171 toxicity is oxidative stress, as already described for TiO_2-NPs in lung and intestinal models (Johnston, 2009; McCracken, 2016; Shi, 2013).

In contrast to the effects on DNA, exposure to E171 only induced minor changes in the expression levels of UPR markers, leading to an overall decrease. Consequently, ER stress was not triggered in our conditions. This finding is in contradiction with previous reports related to *in vivo* and *in vitro* exposure of lung models to TiO_2-NPs (Yu, 2015; Yu, 2015). This apparent discrepancy can be explained by differences in exposure conditions and cell models (lung vs. intestinal), by the physico-chemical characteristics of the TiO_2 particles, and by the doses to which cells were exposed (higher in Yu et al. (Yu, 2015)). In the present study, the overall response of cells to TiO_2-NPs (mostly anatase) was the same as the overall response to E171 (pure anatase), although it was less intense. This could be surprising because NPs with smaller diameter and larger SSA generally trigger a more intense response than larger ones with smaller SSA. However, here the cellular response correlates well with intracellular accumulation of Ti, itself well correlated with the size of TiO_2 agglomerates in exposure medium. Agglomerates of E171 are larger and consequently settle down more quickly than agglomerates of TiO_2-NPs, leading to higher cell exposure level which explains higher cell response.

Repeated exposure to E171 systematically induced more intense cellular responses than acute exposure. This difference in response was not unexpected as in the repeated exposure regimen, cells received 10 or 50 µg/mL of E171 twice a week for 3 weeks, which corresponds to eight times more particles than in the acute exposure condition. And indeed intracellular accumulation of Ti was higher in repeatedly-exposed cells than in acutely-exposed cells. It should be noted that the cells were not subcultured during the 3 weeks of exposure, and therefore the same cells were present from the beginning of the exposure period to the end, progressively accumulating particles. The higher response in repeatedly-exposed cells could also be explained by the fact that, in the repeated exposure regimen, cells are exposed throughout the whole process of their differentiation, and thus on the first day of exposure, they are undifferentiated. Previous studies reported that undifferentiated cells are more sensitive to NPs and accumulate more NPs than differentiated cells (Gerloff, 2013; Song, 2015). E171 could accumulate more intensively during the first week of the repeated exposure regimen, before Caco-2 cells differentiate. Another possible explanation would be that repeated exposure to TiO_2 impairs or delays the process of cell differentiation. Consequently exposed cells would remain undifferentiated for a longer period of time than control cells, which would lead to increased accumulation of particles. However after 21 days of repeated exposure to TiO_2 the morphology of tight junctions and microvilli is similar in exposed cells and in control cells. Moreover qualitative inspection of the Caco-2/HT29-MTX coculture, after repeated exposure to 10 or 50 µg/mL of TiO_2 particles, shows that mucus secretion is similar in repeatedly-exposed cells. These observations suggest that the differentiation process is not drastically affected. Cellular responses to continuous vs. acute exposure to NPs have also been compared in other studies. Some of these studies report similar or higher responses in continuously-exposed cells compared to acutely-exposed cells (Annangi, 2015; Armand, 2016; Armand, 2016; Kocbek, 2010; Vales, 2015), while others indicate lower or

different types of responses in continuously-exposed cells (Annangi, 2016; Aude-Garcia, 2016; Comfort, 2014). A diminished and altered response is always reported for cells continuously exposed to sub-lethal concentrations of NPs that are prone to dissolution or physico-chemical transformation, such as ZnO-NPs (Annangi, 2016) or Ag-NPs (Aude-Garcia, 2016; Comfort, 2014). This effect can be explained by the fact that NP dissolution would lead to the release of toxic metal ions from cells, thus limiting their toxic impact. Transformed NPs show altered surface reactivity, surface coating and/or agglomeration states. Cells chronically exposed to NPs that are prone to transformation would thus be continuously exposed to a mixture of intact and transformed NPs, and the impact of such exposure undoubtedly differs from the impact of exposure to intact NPs alone. In contrast, continuous exposure to insoluble or inert particles, such as TiO_2, could lead to cell overload that may impair normal cellular function and eventually lead to cell death. This raises the question of whether an acute *in vitro* exposure regime can appropriately mimic the chronic *in vivo* exposure situation.

As demonstrated previously for inhalation exposure, acute *in vitro* experiments rarely reproduce the effects observed *in vivo* (Sayes, 2007; Warheit, 2009). Attempts to increase the predictive capacity of *in vitro* models consist in extending the exposure time, reducing the exposure concentration, and applying NPs to cells only for a limited amount of time per day, as would be the case in *in vivo* protocols. Comfort et al. (Comfort, 2014) developed an *in vitro* model of chronic exposure to Ag-NPs, mimicking the protocols used for inhalation exposure, by exposing HaCat cells for 14 weeks to low concentrations of Ag-NPs (pg/mL) for 8 h per day, 5 days per week, and sub-culturing them weekly. Chronically exposed cells showed higher stress than acutely exposed cells, but caused no impact on cell viability. No similar development has been performed to test the effect of oral exposure. We previously compared the *in vitro* response of acutely-exposed intestinal models to the response observed in mice

receiving TiO_2-NPs orally (Brun, 2014). One of the conclusions of this previous study was that *in vitro* cells were more resistant to TiO_2-NPs than the cells in the mouse gut, i.e., the same type of response was observed (including altered cell junctions, leading to altered intestinal permeability), but the responses to *in vitro* and *in vivo* exposures differed in intensity (Brun, 2014). Daily consumption of additive-containing food consists in ingesting the additive once a day, incorporated in a food matrix. As the food matrix passes through the stomach, it is transformed and some elements are removed. The additive would certainly have become coated with some components of this transformed matrix by the time it reaches the intestine. Due to peristaltic movements, the additive then passes through the intestine before it is eliminated. However, some of the additive could be trapped in the intestinal mucus for longer periods of time. In the worst-case scenario, additive trapped in the intestinal mucus would be in continuous contact with epithelial cells. *In vitro*, a repeated exposure scenario where cells are exposed to the food additive three times a week for 3 weeks is therefore a good approximation of this worst-case *in vivo* scenario. Consequently, even if refinements may be required, such as lower E171 concentrations, we believe that the *in vitro* exposure regimen used in this study is a good approximation for the *in vivo* situation.

Finally, the response of both cell models to E171 exposure was fairly similar, although for some endpoints the response was slightly more intense in Caco-2 cells than in the coculture model, which differs from Caco-2 monoculture due to the presence of mucus. Since the coculture is composed of 70% Caco-2 cells, it is not surprising that its response only minimally differs from that of the monoculture (100% Caco-2 cells). The slightly lower sensitivity of the mucus-containing model could be explained by a lower exposure level, because the mucus could trap some particles and prevent them from reaching cell membranes. Depending on their surface charge, particles can be repulsed by the mucus layer, accumulate inside it, or cross it (Frohlich, 2012). In the present study, the two models accumulated similar

amount of Ti, consequently E171 and TiO_2-NPs can cross the mucus layer. The lower sensitivity of the coculture therefore rather relies on a lower intrinsic sensitivity of the coculture model. The mucus layer can be protective by a mechanism which does not involve physical hindrance of particle interaction with cells. Potentially, the mucus provides cells with essential nutrients that enhance their defensive capacity. Moreover some mucins and glycoproteins, especially MUC1, can modulate epithelial cell inflammatory signaling (McGuckin, 2011). MUC1 also protect adenocarcinoma cells from apoptosis, after exposure to genotoxic agents (McGuckin, 2011). The coculture model, which produces MUC1, would therefore respond differently to the well-documented pro-inflammatory potential of TiO_2 particles (Shi, 2013) than the monoculture model, and would potentially be protected from their DNA-damaging action.

Conclusion

The results of this study demonstrate that E171 is only moderately toxic to two intestinal cell models *in vitro*. This toxicity is mainly due to oxidative stress, which results in intracellular ROS accumulation and oxidation of DNA bases; no ER stress or effects on cell viability were observed. Both cell models responded similarly to E171, with a more intense cellular response observed in cells repeatedly exposed to E171 over 21 days, compared to cells exposed to an acute dose for 6 h, 24 h or 48 h. The toxic effects therefore increase as TiO_2 accumulates in intestinal cells, and the presence of a mucus coating on intestinal cells only slightly mitigates these effects. These findings underline the necessity to use repeated exposure regimens rather than acute exposure to correctly assess the mechanisms behind particle and nanoparticle toxicity.

Acknowledgments

This work was supported by the French Atomic Energy and Alternative Energies Commission (CEA) through the 'Toxicology' research program, the French Environment and Energy Management Agency (ADEME), the French Agency for Food, Environmental and Occupational Health & Safety (ANSES) within the framework of the National Research Program for Environmental and Occupational Health (ANSES, Nanogut project) [EST-2013/1/024] and the French National Research Agency (ANR, PAIPITO project) [ANR-16-CE34-0011-01]. This study is a contribution to the Labex Serenade [ANR-11-LABX-0064] funded by the French Government's "Investissements d'Avenir" program through the A*MIDEX project [ANR-11-IDEX-0001-02]. The authors would like to thank T. Lesuffleur (INSERM U938, Paris, France) for her generous gift of HT29-MTX cells, and T. Rabilloud (CNRS, Grenoble, France) for helpful discussions. The authors would like to thank M. Gallagher-Gambarelli, TWS Consulting (Saint-Egreve, France), for English proofreading.

Disclosure of interest

The authors report no conflicts of interest

References

Al-Rasheed NM, Faddah LM, Mohamed AM, Abdel Baky NA, Al-Rasheed NM, Mohammad RA. 2013. Potential impact of quercetin and idebenone against immuno- inflammatory and oxidative renal damage induced in rats by titanium dioxide nanoparticles toxicity. J Oleo Sci 62(11): 961-71.

Amenta V, Aschberger K, Arena M, Bouwmeester H, Botelho Moniz F, Brandhoff P, Gottardo S, Marvin HJ, Mech A, Quiros Pesudo L, Rauscher H, Schoonjans R, Vettori MV, Weigel S, Peters RJ. 2015. Regulatory aspects of nanotechnology in the agri/feed/food sector in EU and non-EU countries. Regul Toxicol Pharmacol 73(1): 463-76.

Annangi B, Bach J, Vales G, Rubio L, Marcos R, Hernandez A. 2015. Long-term exposures to low doses of cobalt nanoparticles induce cell transformation enhanced by oxidative damage. Nanotoxicology 9(2): 138-47.

Annangi B, Rubio L, Alaraby M, Bach J, Marcos R, Hernandez A. 2016. Acute and long-term in vitro effects of zinc oxide nanoparticles. Arch Toxicol 90(9): 2201-13.

Armand L, Biola-Clier M, Bobyk L, Collin-Faure V, Diemer H, Strub JM, Cianferani S, Van Dorsselaer A, Herlin-Boime N, Rabilloud T, Carriere M. 2016. Molecular responses of alveolar epithelial A549 cells to chronic exposure to titanium dioxide nanoparticles: A proteomic view. J Proteomics 134: 163-73.

Armand L, Tarantini A, Beal D, Biola-Clier M, Bobyk L, Sorieul S, Pernet-Gallay K, Marie-Desvergne C, Lynch I, Herlin-Boime N, Carriere M. 2016. Long-term exposure of A549 cells to titanium dioxide nanoparticles induces DNA damage and sensitizes cells towards genotoxic agents. Nanotoxicology 10(7): 913-23.

Aude-Garcia C, Villiers F, Collin-Faure V, Pernet-Gallay K, Jouneau PH, Sorieul S, Mure G, Gerdil A, Herlin-Boime N, Carriere M, Rabilloud T. 2016. Different in vitro exposure

regimens of murine primary macrophages to silver nanoparticles induce different fates of nanoparticles and different toxicological and functional consequences. Nanotoxicology 10(5): 586-96.

Bettini S, Boutet-Robinet E, Cartier C, Comera C, Gaultier E, Dupuy J, Naud N, Tache S, Grysan P, Reguer S, Thieriet N, Refregiers M, Thiaudiere D, Cravedi JP, Carriere M, Audinot JN, Pierre FH, Guzylack-Piriou L, Houdeau E. 2017. Food-grade TiO2 impairs intestinal and systemic immune homeostasis, initiates preneoplastic lesions and promotes aberrant crypt development in the rat colon. Sci Rep 7: 40373.

Brun E, Barreau F, Veronesi G, Fayard B, Sorieul S, Chaneac C, Carapito C, Rabilloud T, Mabondzo A, Herlin-Boime N, Carriere M. 2014. Titanium dioxide nanoparticle impact and translocation through ex vivo, in vivo and in vitro gut epithelia. Part Fibre Toxicol 11: 13.

Carriere M, Sauvaigo S, Douki T, Ravanat JL. 2017. Impact of nanoparticles on DNA repair processes: current knowledge and working hypotheses. Mutagenesis 32(1): 203-213.

Chaudhari N, Talwar P, Parimisetty A, Lefebvre d'Hellencourt C, Ravanan P. 2014. A molecular web: endoplasmic reticulum stress, inflammation, and oxidative stress. Front Cell Neurosci 8: 213.

Chen XX, Cheng B, Yang YX, Cao A, Liu JH, Du LJ, Liu Y, Zhao Y, Wang H. 2013. Characterization and preliminary toxicity assay of nano-titanium dioxide additive in sugar-coated chewing gum. Small 9(9-10): 1765-74.

Chen Z, Wang Y, Zhuo L, Chen S, Zhao L, Luan X, Wang H, Jia G. 2015. Effect of titanium dioxide nanoparticles on the cardiovascular system after oral administration. Toxicol Lett 239(2): 123-30.

Comfort KK, Braydich-Stolle LK, Maurer EI, Hussain SM. 2014. Less is more: long-term in vitro exposure to low levels of silver nanoparticles provides new insights for nanomaterial evaluation. ACS Nano 8(4): 3260-71.

Deuring JJ, Peppelenbosch MP, Kuipers EJ, van der Woude CJ, de Haar C. 2011. Impeded protein folding and function in active inflammatory bowel disease. Biochem Soc Trans 39(4): 1107-11.

Dorier M, Brun E, Veronesi G, Barreau F, Pernet-Gallay K, Desvergne C, Rabilloud T, Carapito C, Herlin-Boime N, Carriere M. 2015. Impact of anatase and rutile titanium dioxide nanoparticles on uptake carriers and efflux pumps in Caco-2 gut epithelial cells. Nanoscale 7(16): 7352-60.

EFSA AP. 2016. Scientific Opinion on the re-evaluation of titanium dioxide (E 171) as a food additive. EFSA Journal 14(9): 4545-4628.

Frohlich E, Roblegg E. 2012. Models for oral uptake of nanoparticles in consumer products. Toxicology 291(1-3): 10-7.

Gerloff K, Fenoglio I, Carella E, Kolling J, Albrecht C, Boots AW, Forster I, Schins RP. 2012. Distinctive toxicity of TiO2 rutile/anatase mixed phase nanoparticles on Caco-2 cells. Chem Res Toxicol 25(3): 646-55.

Gerloff K, Pereira DI, Faria N, Boots AW, Kolling J, Forster I, Albrecht C, Powell JJ, Schins RP. 2013. Influence of simulated gastrointestinal conditions on particle-induced cytotoxicity and interleukin-8 regulation in differentiated and undifferentiated Caco-2 cells. Nanotoxicology 7(4): 353-66.

Grande F, Tucci P. 2016. Titanium Dioxide Nanoparticles: a Risk for Human Health? Mini Rev Med Chem 16(9): 762-9.

Heringa MB, Geraets L, van Eijkeren JC, Vandebriel RJ, de Jong WH, Oomen AG. 2016. Risk assessment of titanium dioxide nanoparticles via oral exposure, including toxicokinetic considerations. Nanotoxicology: 1-11.

Jia F, Sun Z, Yan X, Zhou B, Wang J. 2014. Effect of pubertal nano-TiO2 exposure on testosterone synthesis and spermatogenesis in mice. Arch Toxicol 88(3): 781-8.

Johnston HJ, Hutchison GR, Christensen FM, Peters S, Hankin S, Stone V. 2009. Identification of the mechanisms that drive the toxicity of TiO2 particulates: the contribution of physicochemical characteristics. Particle and Fibre Toxicology 6.

Jovanovic B. 2015. Critical review of public health regulations of titanium dioxide, a human food additive. Integr Environ Assess Manag 11(1): 10-20.

Jugan ML, Barillet S, Simon-Deckers A, Herlin-Boime N, Sauvaigo S, Douki T, Carriere M. 2012. Titanium dioxide nanoparticles exhibit genotoxicity and impair DNA repair activity in A549 cells. Nanotoxicology 6(5): 501-13.

Kocbek P, Teskac K, Kreft ME, Kristl J. 2010. Toxicological aspects of long-term treatment of keratinocytes with ZnO and TiO2 nanoparticles. Small 6(17): 1908-17.

Lesuffleur T, Barbat A, Dussaulx E, Zweibaum A. 1990. Growth adaptation to methotrexate of HT-29 human colon carcinoma cells is associated with their ability to differentiate into columnar absorptive and mucus-secreting cells. Cancer Res 50(19): 6334-43.

Lesuffleur T, Porchet N, Aubert JP, Swallow D, Gum JR, Kim YS, Real FX, Zweibaum A. 1993. Differential expression of the human mucin genes MUC1 to MUC5 in relation to growth and differentiation of different mucus-secreting HT-29 cell subpopulations. J Cell Sci 106 (Pt 3): 771-83.

Malhotra JD, Kaufman RJ. 2007. Endoplasmic reticulum stress and oxidative stress: a vicious cycle or a double-edged sword? Antioxid Redox Signal 9(12): 2277-93.

McCracken C, Dutta PK, Waldman WJ. 2016. Critical assessment of toxicological effects of ingested nanoparticles. Environmental Science-Nano 3(2): 256-282.

McGuckin MA, Linden SK, Sutton P, Florin TH. 2011. Mucin dynamics and enteric pathogens. Nat Rev Microbiol 9(4): 265-78.

Pele LC, Thoree V, Bruggraber SF, Koller D, Thompson RP, Lomer MC, Powell JJ. 2015. Pharmaceutical/food grade titanium dioxide particles are absorbed into the bloodstream of human volunteers. Part Fibre Toxicol 12: 26.

Peters RJ, van Bemmel G, Herrera-Rivera Z, Helsper HP, Marvin HJ, Weigel S, Tromp PC, Oomen AG, Rietveld AG, Bouwmeester H. 2014. Characterization of titanium dioxide nanoparticles in food products: analytical methods to define nanoparticles. J Agric Food Chem 62(27): 6285-93.

Pfaffl MW, Horgan GW, Dempfle L. 2002. Relative expression software tool (REST) for group-wise comparison and statistical analysis of relative expression results in real-time PCR. Nucleic Acids Res 30(9): e36.

Pfaffl MW, Tichopad A, Prgomet C, Neuvians TP. 2004. Determination of stable housekeeping genes, differentially regulated target genes and sample integrity: BestKeeper--Excel-based tool using pair-wise correlations. Biotechnol Lett 26(6): 509-15.

Pignon B, Maskrot H, Ferreol VG, Leconte Y, Coste S, Gervais M, Pouget T, Reynaud C, Tranchant JF, Herlin-Boime N. 2008. Versatility of laser pyrolysis applied to the synthesis of TiO2 nanoparticles - Application to UV attenuation. European Journal of Inorganic Chemistry(6): 883-889.

Powell JJ, Faria N, Thomas-McKay E, Pele LC. 2010. Origin and fate of dietary nanoparticles and microparticles in the gastrointestinal tract. J Autoimmun 34(3): J226-33.

Rompelberg C, Heringa MB, van Donkersgoed G, Drijvers J, Roos A, Westenbrink S, Peters R, van Bemmel G, Brand W, Oomen AG. 2016. Oral intake of added titanium dioxide and its nanofraction from food products, food supplements and toothpaste by the Dutch population. Nanotoxicology 10(10): 1404-1414.

Sayes CM, Reed KL, Warheit DB. 2007. Assessing toxicity of fine and nanoparticles: comparing in vitro measurements to in vivo pulmonary toxicity profiles. Toxicol Sci 97(1): 163-80.

Shi H, Magaye R, Castranova V, Zhao J. 2013. Titanium dioxide nanoparticles: a review of current toxicological data. Part Fibre Toxicol 10: 15.

Simon-Deckers A, Gouget B, Mayne-L'hermite M, Herlin-Boime N, Reynaud C, Carriere M. 2008. In vitro investigation of oxide nanoparticle and carbon nanotube toxicity and intracellular accumulation in A549 human pneumocytes. Toxicology 253(1-3): 137-46.

Skocaj M, Filipic M, Petkovic J, Novak S. 2011. Titanium dioxide in our everyday life; is it safe? Radiol Oncol 45(4): 227-47.

Song ZM, Chen N, Liu JH, Tang H, Deng X, Xi WS, Han K, Cao A, Liu Y, Wang H. 2015. Biological effect of food additive titanium dioxide nanoparticles on intestine: an in vitro study. J Appl Toxicol 35(10): 1169-78.

Taurozzi JS, Hackley VA, Wiesner MR. 2011. Ultrasonic dispersion of nanoparticles for environmental, health and safety assessment--issues and recommendations. Nanotoxicology 5(4): 711-29.

Tay CY, Fang W, Setyawati MI, Chia SL, Tan KS, Hong CH, Leong DT. 2014. Nano-hydroxyapatite and nano-titanium dioxide exhibit different subcellular distribution and apoptotic profile in human oral epithelium. ACS Appl Mater Interfaces 6(9): 6248-56.

Tice RR, Agurell E, Anderson D, Burlinson B, Hartmann A, Kobayashi H, Miyamae Y, Rojas E, Ryu JC, Sasaki YF. 2000. Single cell gel/comet assay: guidelines for in vitro and in vivo genetic toxicology testing. Environ Mol Mutagen 35(3): 206-21.

Urrutia-Ortega IM, Garduno-Balderas LG, Delgado-Buenrostro NL, Freyre-Fonseca V, Flores-Flores JO, Gonzalez-Robles A, Pedraza-Chaverri J, Hernandez-Pando R, Rodriguez-Sosa M, Leon-Cabrera S, Terrazas LI, van Loveren H, Chirino YI. 2016. Food-grade titanium dioxide exposure exacerbates tumor formation in colitis associated cancer model. Food and Chemical Toxicology 93: 20-31.

Vales G, Rubio L, Marcos R. 2015. Long-term exposures to low doses of titanium dioxide nanoparticles induce cell transformation, but not genotoxic damage in BEAS-2B cells. Nanotoxicology 9(5): 568-78.

Wang J, Zhou G, Chen C, Yu H, Wang T, Ma Y, Jia G, Gao Y, Li B, Sun J, Li Y, Jiao F, Zhao Y, Chai Z. 2007. Acute toxicity and biodistribution of different sized titanium dioxide particles in mice after oral administration. Toxicol Lett 168(2): 176-85.

Wang Y, Chen Z, Ba T, Pu J, Chen T, Song Y, Gu Y, Qian Q, Xu Y, Xiang K, Wang H, Jia G. 2013. Susceptibility of young and adult rats to the oral toxicity of titanium dioxide nanoparticles. Small 9(9-10): 1742-52.

Warheit DB, Brown SC, Donner EM. 2015. Acute and subchronic oral toxicity studies in rats with nanoscale and pigment grade titanium dioxide particles. Food Chem Toxicol 84: 208-24.

Warheit DB, Sayes CM, Reed KL. 2009. Nanoscale and fine zinc oxide particles: can in vitro assays accurately forecast lung hazards following inhalation exposures? Environ Sci Technol 43(20): 7939-45.

Weir A, Westerhoff P, Fabricius L, Hristovski K, von Goetz N. 2012. Titanium dioxide nanoparticles in food and personal care products. Environ Sci Technol 46(4): 2242-50.

Yang Y, Doudrick K, Bi X, Hristovski K, Herckes P, Westerhoff P, Kaegi R. 2014. Characterization of food-grade titanium dioxide: the presence of nanosized particles. Environ Sci Technol 48(11): 6391-400.

Yu KN, Chang SH, Park SJ, Lim J, Lee J, Yoon TJ, Kim JS, Cho MH. 2015. Titanium Dioxide Nanoparticles Induce Endoplasmic Reticulum Stress-Mediated Autophagic Cell Death via Mitochondria-Associated Endoplasmic Reticulum Membrane Disruption in Normal Lung Cells. PLoS One 10(6): e0131208.

Yu KN, Sung JH, Lee S, Kim JE, Kim S, Cho WY, Lee AY, Park SJ, Lim J, Park C, Chae C, Lee JK, Lee J, Kim JS, Cho MH. 2015. Inhalation of titanium dioxide induces endoplasmic reticulum stress-mediated autophagy and inflammation in mice. Food Chem Toxicol 85: 106-13.

Zhang K, Kaufman RJ. 2008. From endoplasmic-reticulum stress to the inflammatory response. Nature 454(7203): 455-62.

Table 1. Physico-chemical characteristics of E171A and TiO_2-NPs[a]

	diam. (nm)	SSA (m^2/g)	Crystal. struct.	H. diam. water (nm)	PdI water	ζ medium (mV)	HD med., 0 h (nm)	PdI med., 0 h	HD med., 48 h (nm)	PdI med., 48 h
E171A	118±53	9.4	>95% anat.	415.4±69.5	0.48±0.071	-19±0.7	739.3±355.3	0.64±0.22	777.7 ± 405.2	0.70±0.25
A12	12±3	82	>95% anat.	85±2.9	0.17±0.021	-10.8±0.6	447.9±0.3	0.25±0.01	423.5 ± 3.5	0.33±0.12
P25	24±6	46	86% anat.	157.6±1.0	0.16±0.012	-11.2±0.8	439.9±6.7	0.18±0.01	432.4 ± 8.5	0.23±0.05

[a]Primary diameter (diam.) was measured on TEM images (the diameter of 200-500 particles was manually measured), specific surface area (SSA) was determined using the Brunauer, Emmett and Teller (BET) method. Crystalline structure (cryst. struct.) was identified by X-ray diffraction. Hydrodynamic diameters (HD), mean±standard deviation, corresponds to the Z-average values given by the Nanosizer; PdI, polydispersity indexes. HD measurements were performed in ultrapure water (water) or in cell culture medium (med.). The zeta potential (ζ) was measured in cell culture medium before cell exposure.

Table 2. Quantification of cellular Ti content[a]

	Caco-2			Caco-2/HT29-MTX		
	6 h	48 h	21 d	6 h	48 h	21 d
CTL	0.02±0.03	0.01±0.01	0.01±0.01	0.01±0.01	0.01±0.01	0.01±0.01
A12	0.11±0.05	0.15±0.08*	1.37±0.35$^{*,\#}$	0.19±0.07*	0.08±0.05*	1.59±0.17$^{*,\#}$
P25	1.63±0.64*	4.67±0.34$^{*,\$}$	14.33±0.43$^{*,\#}$	n/a	1.48±0.18*	11.72±0.59$^{*,\#}$
E171	3.26±1.64*	6.93±2.15$^{*,\$}$	27.67±3.07$^{*,\#}$	5.06±2.19*	4.60±2.44*	40.13±10.24$^{*,\#}$

[a]Ti concentrations (µg/L) measured by ICP-MS in Caco-2 and Caco-2/HT29-MTX cells exposed to 50 µg/mL of A12, P25 or E171 for 6 h, 48 h or repeatedly for 21 days. Statistical significance, $P<0.05$, *: exposed vs. control (CTL), $: 6 h vs. 48 h, #: 48 h vs. 21 days. Caco-2 vs. Caco-2/HT29-MTX: none of the differences were statistically significant. The experiment was performed once, with three independent replicates. n/a: not available.

Table 3. Chronic exposure to TiO_2 induces DNA damage[a]

	Caco-2		Caco-2/HT29-MTX	
	Alkaline	+Fpg	Alkaline	+Fpg
A12, 10 µg/mL	2.1±0.9	1.2±0.2	1.4±0.1	1.4±0.1
A12, 50 µg/mL	0.8±0.0	1.3±0.3	0.9±0.1	0.7±0.3
P25, 10 µg/mL	0.7±0.4	1.3±0.1	1.3±0.5	1.0±0.1
P25, 50 µg/mL	0.7±0.5	1.2±0.2	0.8±0.4	1.6±0.7
E171, 10 µg/mL	1.3±0.5	2.0±0.1*	0.8±0.3	1.6±0.9
E171, 50 µg/mL	1.7±0.9	2.1±0.8*	0.7±0.4	2.0±0.8*

[a] %tail DNA expressed as fold-change compared to %tail DNA in control cells, as measured by the alkaline version (alkaline) or the Fpg-modified version (+Fpg) of the comet assay, after chronic exposure of the two cell models to TiO_2 in different forms. Results are expressed as average ± standard deviation of three independent experiments, *$p<0.05$, exposed vs control, n=3.

Figure 1.

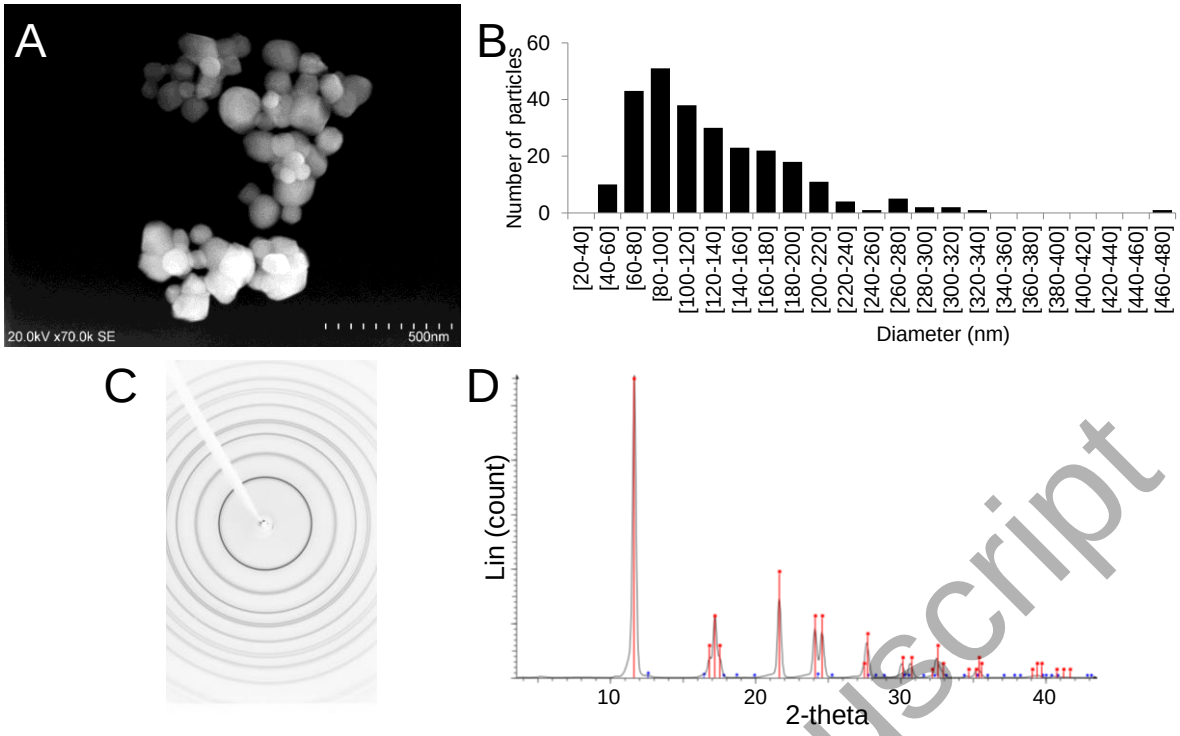

Figure 2.

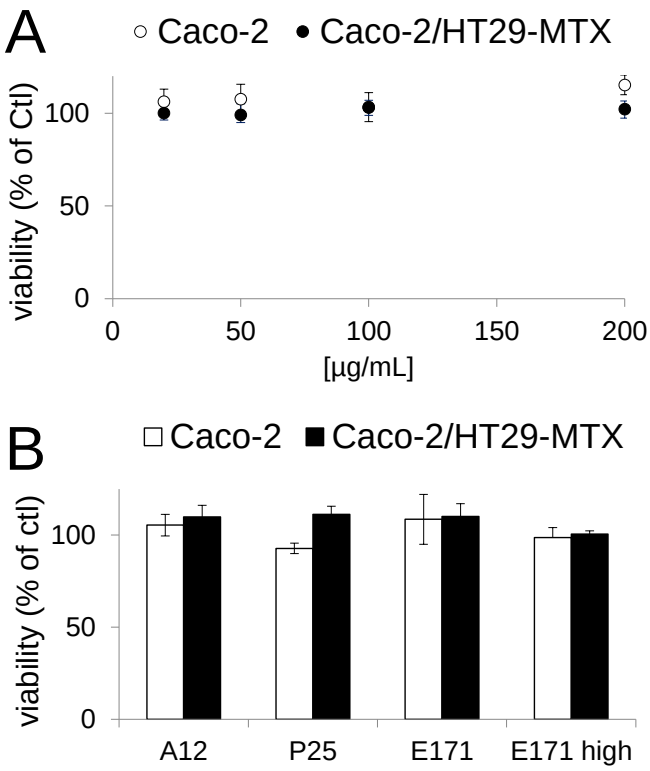

Figure 3.

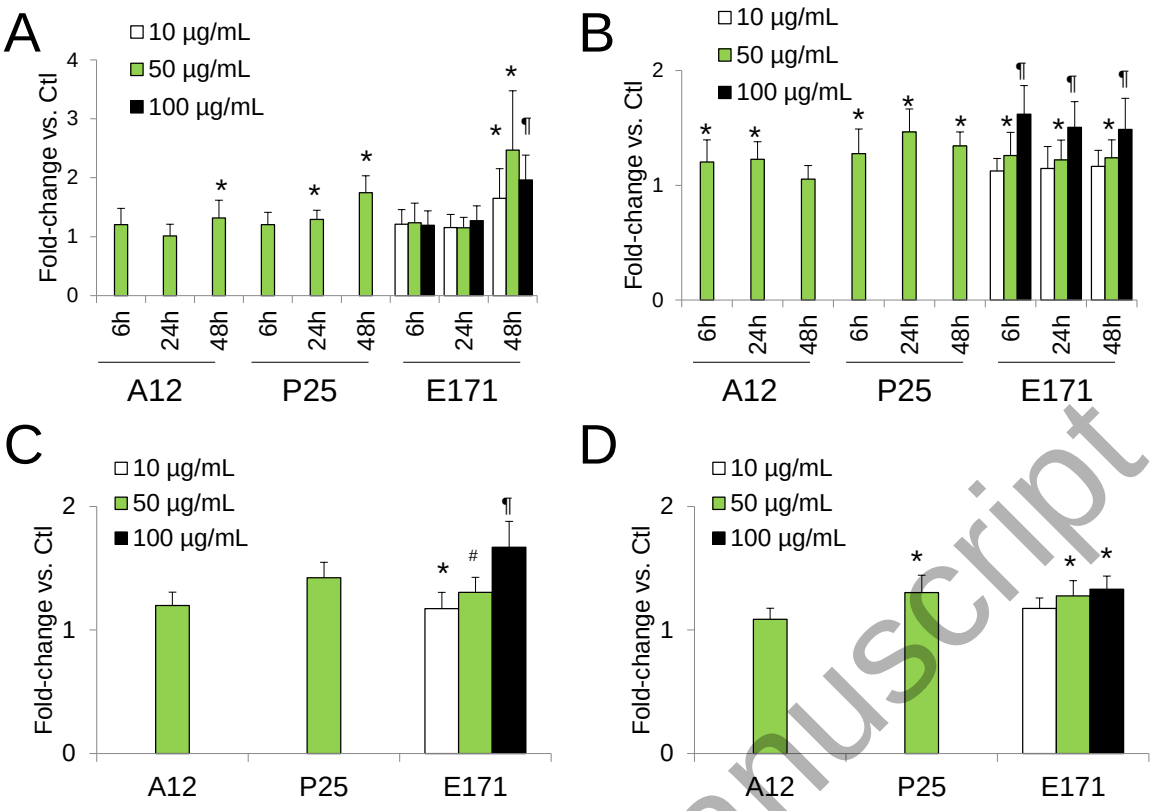

Figure 4.

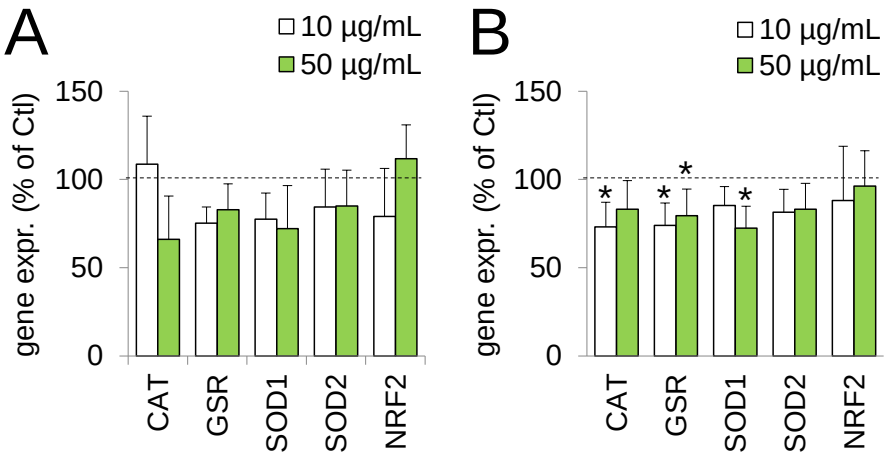

Figure 5.

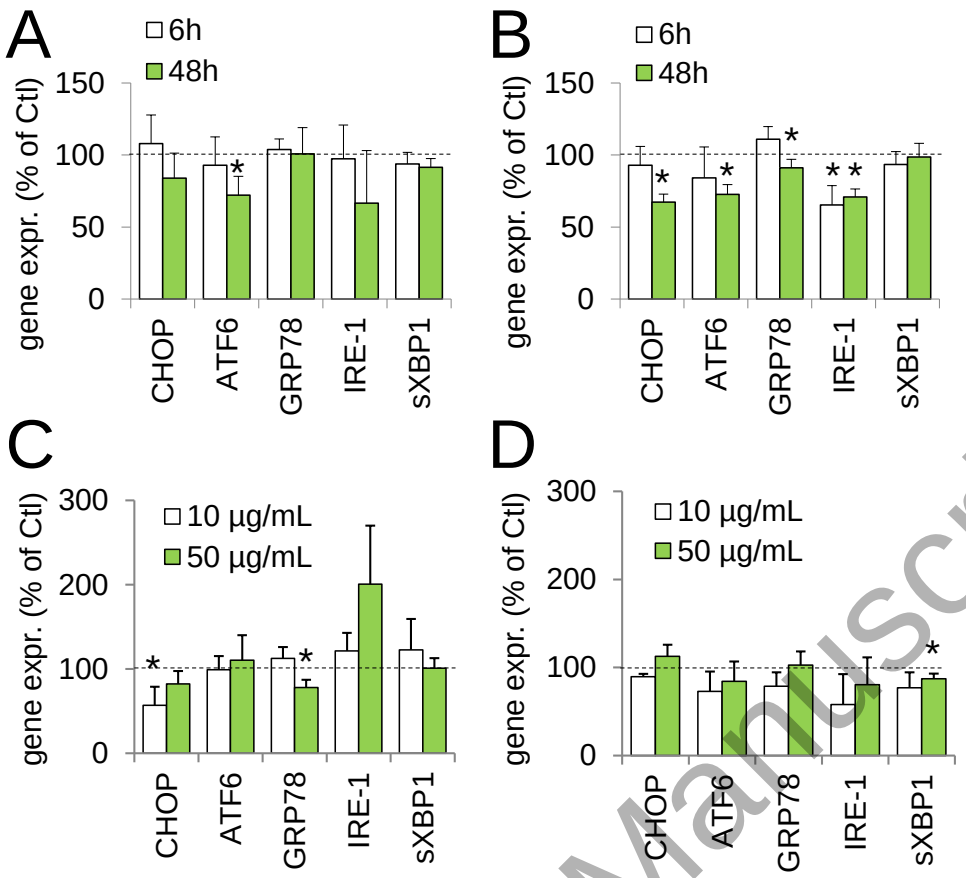

Figure legends

Figure 1. Physico-chemical characterization of E171. (A) Scanning electron microscopy image of E171 recorded in secondary electron mode; (B) primary size distribution calculated based on diameters measured on TEM images (depending on the sample, the diameter of 200-500 particles was manually measured). (C-D) X-ray diffraction analysis of E171 powder; the main diffraction lines of anatase are indicated in red and the main diffraction lines of rutile are indicated in blue.

Figure 2. Exposure to TiO_2-NPs does not alter cell viability. (A) cell viability after 48 h of acute exposure to E171 assessed using the WST1 assay; (B) cell viability in cells repeatedly exposed to 10 µg/mL of A12, P25 or E171 ("A12", "P25" and "E171") or to 50 µg/mL of E171 ("E171 high"), as determined using trypan blue (Caco-2) or IP (Caco-2/HT29-MTX) exclusion assays. % of control (Ctl) (unexposed cells), mean±standard deviation, n=3.

Figure 3. Exposure to TiO_2-NPs increases intracellular ROS levels. ROS were quantified using H2-DCF-DA, in Caco-2 cells (A, C) and Caco-2/HT29-MTX coculture (B, D) after acute exposure for 6 h, 24 h or 48 h (A, B), or repeated exposure over 21 days (C, D). Results are expressed as fold-increase vs. control (unexposed cells), mean±standard deviation, *P<0.05 vs. Ctl, $^{\#}$P<0.05 vs. Ctl and 10 µg/mL, ¶P<0.05 vs. Ctl and 50 µg/mL, n=4.

Figure 4. Expression of antioxidant enzymes altered in cells repeatedly exposed to E171. RT-qPCR was performed in Caco-2 (A) and Caco-2/HT29-MTX (B) models after repeated exposure for 21 days to 10 or 50 µg/mL of E171, and compared to the respective control (unexposed Caco-2 monoculture and unexposed Caco-2/HT29-MTX coculture). The genes tested were catalase (*CAT*), glutathione reductase (*GSR*), superoxide dismutases 1 and 2

(*SOD1*, *SOD2*) and nuclear factor (erythroid-derived 2)-like 2 (*NRF2*). Results are expressed as fold-increase vs. control (unexposed cells), mean±standard deviation, *P<0.05, n=3.

Figure 5. Reduced expression of some ER stress markers in cells exposed to E171. RT-qPCR was performed in Caco-2 (A, C) and Caco-2/HT29-MTX (B, D) models after acute exposure to 50 µg/mL of E171 for 6 h or 48 h (A, B), or chronic exposure to 10 or 50 µg/mL of E171 for 21 days (C, D), compared to the respective control (unexposed Caco-2 monoculture and unexposed Caco-2/HT29-MTX coculture). The genes tested were: DNA Damage Inducible Transcript 3 (*CHOP*), Activating Transcription Factor 6 (*ATF6*), Heat Shock Protein Family A (Hsp70) Member 5 (*GRP78*), Endoplasmic Reticulum To Nucleus Signaling 1 (*IRE-1*), X-Box Binding Protein 1 (*sXBP1*). All these genes are involved in the UPR, which is increased in ER stress conditions. Fold-increase vs. control (unexposed cells), mean±standard deviation, *P<0.05, n=3.

Supplemental materials for:

Continuous in vitro exposure of intestinal epithelial cells to E171 food additive causes oxidative stress, inducing oxidation of DNA bases but no endoplasmic reticulum stress

Marie Dorier, David Béal, Caroline Marie-Desvergne, Muriel Dubosson, Frédérick Barreau, Eric Houdeau, Nathalie Herlin-Boime, Marie Carriere

Materials and Methods

Cell model characterization

Mucus secretion

For mucus staining, cells were washed with PBS, fixed in 90% ethanol/3% acetic acid for 20 min at room temperature (RT), stained with 1% (w./v.) Alcian blue, pH 2.5, for 30 min at RT in the dark and under stirring. Cells were then washed twice and imaged with an optical microscope (Axiovert 25 Zeiss). Mucus staining was also performed using Periodic Acid-Schiff (PAS). After fixation, cells were washed with distilled water, incubated for 15 min at RT with Schiff reagent and further washed for 5 min, then incubated for 90 s with the hematoxylin solution. After washing with water, cells were imaged using an optical microscope (Axiovert 25 Zeiss).

Characterization of microvilli

Alkaline phosphatase (ALP) enzymatic activity is typically expressed in microvilli; it may be found in the cell glycocalyx (Sambuy, 2005). ALP activity was imaged and quantified in cells exposed to E171 or TiO_2-NPs. Cells were labeled using the SIGMA *FAST*™ labeling assay after seeding in 60 cm^2 dishes. Briefly, Fast-Red and Tris tablets were dissolved in 10 mL deionized water and mixed. This solution was deposited on the plates containing cells after exposure (or not) to particles. After 1 h of incubation at 37 °C, the reaction was stopped by washing with water. Cells were observed and imaged using an optical microscope (Axiovert 25 Zeiss). To quantify ALP activity, cells were seeded in 24-well plates and ALP activity was measured using a fluorometric assay kit (K422-500, Biovision) according to the manufacturer's procedure with slight modifications. Thus, cells were harvested and counted, then pelleted by centrifugation (250 rcf, 5 min) and washed with PBS. Assay buffer was added and cells were centrifuged for 3 min at 13000 rcf. The supernatant was then deposited in a clean black 96-well plate, in duplicate. Subsequent steps are described in the assay protocol. Fluorescence was measured and normalized for the total number of cells per well (fluorescence unit per cell number). This assay was repeated three times independently.

Transmission electron microscopy

For transmission electron microscopy (TEM) imaging, after exposure to E171, cells were rinsed with PBS, fixed in 2% glutaraldehyde prepared in cacodylate buffer then in 1% osmium tetroxide. They were then dehydrated through a graded series of ethanol and

embedded in Epon resin. Ultra-thin sections were cut and stained with 1% uranyl acetate. They were observed on a JEOL 1200EX TEM operating at 80 kV (Grenoble Institut des Neurosciences, Grenoble, France).

Figure S1. Characterization of cell models. (A) Alcian Blue and Periodic Acid Schiff (PAS) staining of the mucus and alkaline phosphatase staining , in Caco-2/HT29-MTX coculture, and Caco-2 cells. (B) Alkaline phosphatase (ALP) activity measured in Caco-2 cells, Caco-2/HT29-MTX coculture and HT29-MTX monoculture after 21 days of differentiation. Results represent mean fluorescence ± standard deviation, *p<0.05 Caco-2/HT29-MTX or HT29-MTX vs. Caco-2, n=3.

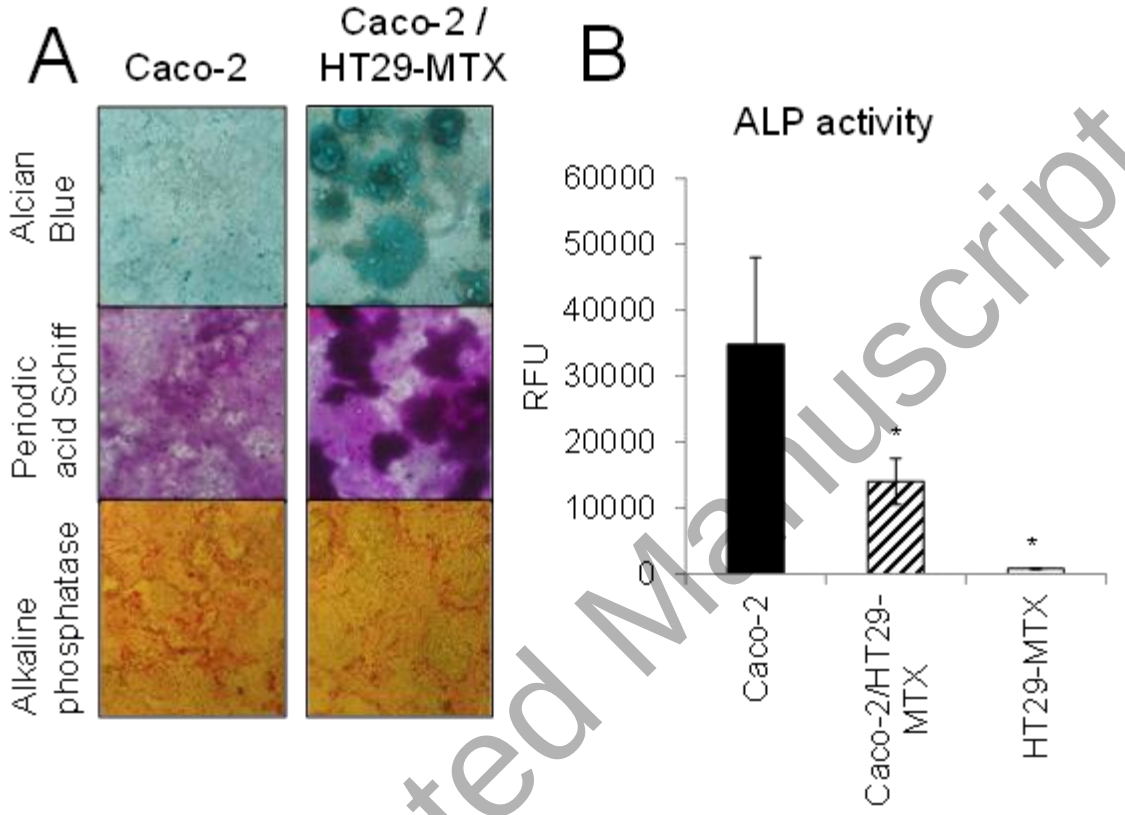

Figure S2. Schematic representation of the exposure protocol. (A, B) Acute exposure: 21 days after seeding differentiated cells were exposed to particles for 6 h, 24 h or 48 h. Cells were either exposed at different times and harvested at simultaneously (A), or exposed simultaneously and harvested at different times (B). (C) Chronic exposure: cells were seeded and exposed to particles at every change of culture medium over the 21 days of their differentiation; the culture medium containing TiO_2 particles was thus renewed eight times from seeding to harvesting.

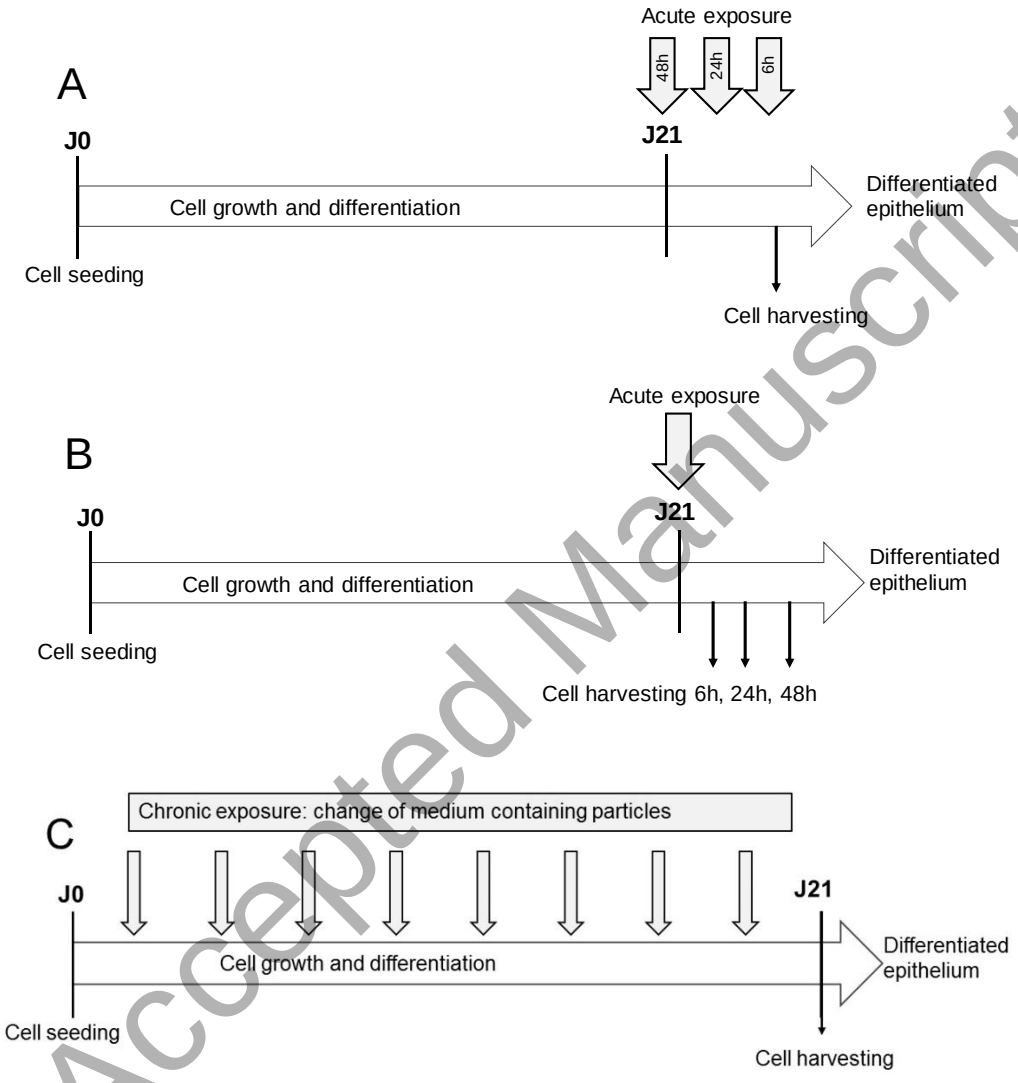

Figure S3. Differentiation status of chronically-exposed Caco-2/HT29-MTX cells. Cells were seeded and exposed to E171 particles at every change of culture medium over the 21 days of their differentiation. The presence of tight junctions (A, arrows; scale bar: 2 µm) and microvilli (B, arrows; cross sections of microvilli appear spherical or spheroidal; scale bar: 2 µm) was observed by TEM in cells chronically exposed to 50 µg/mL of E171. The presence of mucus was imaged under an optical microscope after staining with Alcian Blue, in control cells (C) and cells exposed to 10 (D) or 50 (E) µg/mL of E171.

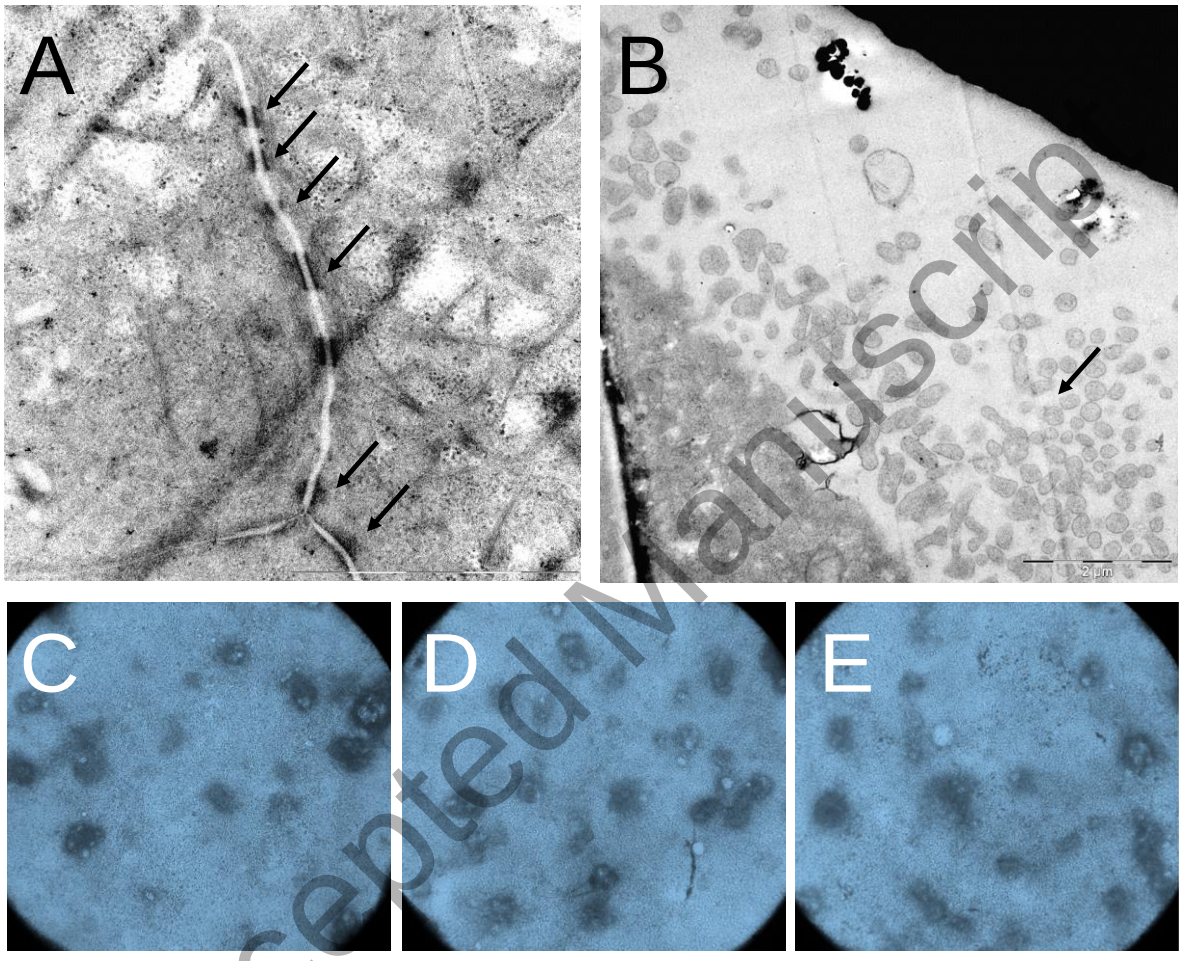

Figure S4. TEM of E171 accumulated in chronically-exposed Caco-2/HT29-MTX cells. Cells were seeded and exposed to 50 µg/mL of E171 particles at every change of culture medium over the 21 days of their differentiation; the culture medium containing TiO_2 particles was thus renewed eight times from seeding to harvesting. n.: nucleus; c.: cytoplasm; e.: extracellular space. Scale bar: (A): 5 µm; (B): 1 µm.

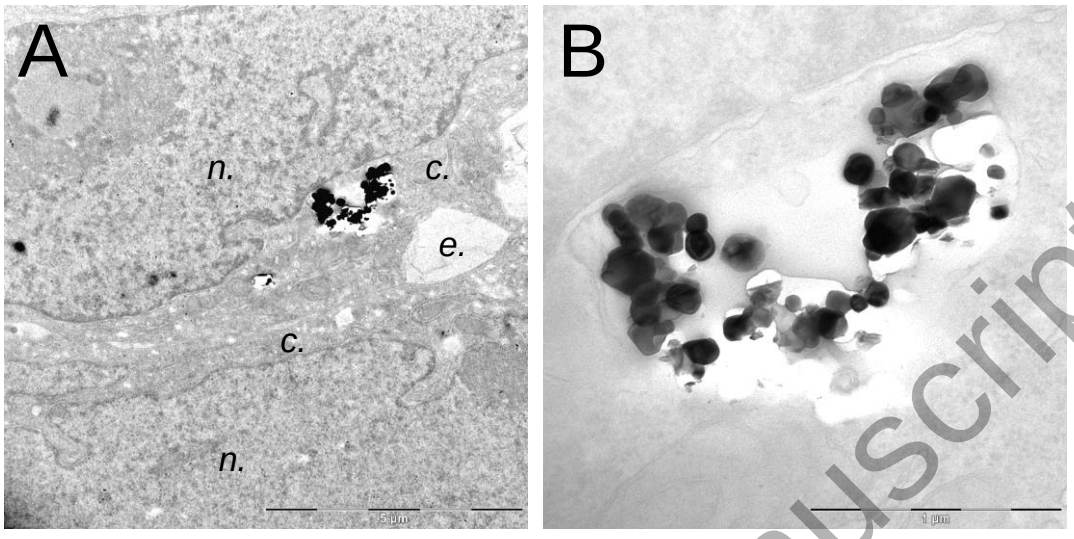

Table S1. Interference of TiO_2 particles with the H2-DCF-DA assay[a]

	Caco-2				Caco-2/HT29-MTX			
	acute	Acute + H_2-DCF-DA	chronic	chronic + H_2-DCF-DA	acute	acute + H_2-DCF-DA	chronic	chronic + H_2-DCF-DA
Control	11.9±2.9	9185.6±915.8	15.4±0.3	3739.2±370.0	17.2±0.3	11643.2±937.7	15.7±0.0	3056.8±145.5
A12 50 µg/mL	9.4±1.1	11758.7±902.1	11.0±1.7	3743.1±195.3	14.6±0.3	11992.4±1213.5	16.5±3.0	3768.0±347.5
P25 50 µg/mL	9.2±0.6	13785.2±131.9	10.5±2.3	5000.0±683.0	14.6±0.9	16646.6±607.0	15.4±0.7	4177.8±613.3
E171 10 µg/mL	10.0±2.1	11662.4±763.2	12.2±0.1	3879.0±194.5	17.1±1.3	14673.4±1454.1	15.7±2.5	3686.1±129.0
E171 50 µg/mL	8.4±1.6	15081.0±1775.0	13.2±0.3	4063.7±102.5	16.5±0.5	14940.1±1697.9	14.7±0.1	4003.4±332.8
E171 100 µg/L	7.9±0.8	14664.9±1770.3	11.2±1.6	4438.9±496.8	14.1±2.3	18843.0±2751.2	14.6±0.5	4208.8±405.5

	PBS + H_2-DCF-DA
Control	2.6±0.1
A12 50 µg/mL	3.3±0.0
P25 50 µg/mL	3.4±0.2
E171 10 µg/mL	2.7±0.2
E171 50 µg/mL	3.2±0.3
E171 100 µg/L	4.1±0.1

[a]Fluorescence was measured with excitation at 480 nm and emission at 530 nm in cells exposed to particles but not H2DCF-DA, or in cells exposed to both particles and H2DCF-DA (upper table). Alternatively, fluorescence was measured in suspensions of particles in which H2DCF-DA was added, i.e. in an acellular system (lower table).

Table S2. Primers used in RT-qPCR experiments

Gene	Forward primer	Reverse primer
CAT	5’-AGC-TTA-GCG-TTC-ATC-CGT-GT-3’	5’-TCC-AAT-CATC-CGT-CAA-AAC-A-3’
GSR	5’-GAT-CCC-AAG-CCC-ACA-ATA-GA-3’	5’-CTT-AGA-ACC-CAG-GGC-TGA-CA-3’
SOD1	5’-AGG-GCA-TCA-TCA-ATT-TCG-AG-3’	5’-ACA-TTG-CCC-AAG-TCT-CCA-AC-3’
SOD2	5’-TCC-ACT-GCA-AGG-AAC-AAC-AG-3’	5’-TCT-TGC-TGG-GAT-CAT-TAG-GG-3’
NRF2	5’-CAG-TCA-GCG-ACG-GAA-AGA-GT-3’	5’-ACC-TGG-GAG-TAG-TTG-GCA-GA-3’
GRP78	5’-GGT-GAA-AGA-CCC-CTG-ACA-AA-3’	5’-GTC-AGG-CGA-TTC-TGG-TCA-TT-3’
CHOP	5’-TGG-AAG-CCT-GGT-ATG-AGG-AC-3’	5’-TGT-GAC-CTC-TGC-TGG-TTC-TG-3’
IRE1	5’-AGA-GAG-GCG-GGA-GAG-CCG-TG-3’	5’-CGA-GGA-GGT-GGG-GGA-AGC-GA-3’
sXBP1	5’-GCA-GGT-GCA-GGC-CCA-GTT-GT-3’	5’-TGG-GTC-CAA-GTT-GTC-CAG-AAT-GC-3’
ATF-6	5’-CCA-GCA-GCA-CCC-AAG-ACT-CAA-ACA-3’	5’-GTG-TGA-CTC-CCC-CAG-CAA-CAG-C-3’

Table S3. Physico-chemical characteristics of the five batches of E171[a]

	SSA (m^2/g)	Theor. Diam. (nm)	Diam. TEM (nm)	%<100 nm	nb	Crystal structure
E171 A	9.4	160	119±65	47	192	anatase
E171 B	12.4	121	117±41	40	200	anatase + traces rutile
E171 C	8.4	180	136±53	30	210	anatase + traces rutile
E171 D	10.8	139	100±36	55	200	anatase
E171 E	11.8	128	109±37	45	150	anatase + traces rutile

[a]Specific surface area (SSA) measured by the Brunauer, Emmett and Teller (BET) method, theoretical mean diameter (Theor. Diam.) determined based on the Sherrer equation, primary diameter (Diam.) and percentage of particles with diameters below 100 nm (%<100 nm), as analyzed using transmission electron microscopy (TEM). Crystalline phase identified by X-ray diffraction (DRX).

Table S4. RT-qPCR analysis of expression levels for redox enzymes[a]

	Caco-2				Caco-2/HT29-MTX			
	6 h 50µg/mL	48 h 50µg/mL	21 days 10 µg/mL	21 days 50 µg/mL	6 h 50µg/mL	48 h 50µg/mL	21 days 10 µg/mL	21 days 50 µg/mL
A12								
CAT	1.02±0.39	0.94±0.2	0.91±0.230	0.96± 0.28	1.2-±0.19	1.29±0.29	0.7±0.16*	0.76±0.16
GSR	0.97±0.31	0.94±0.14	0.81 ±0.12	0.78 ±0.16	1.12±0.14	1.25±0.13*	0.82±0.16	0.8±0.14
SOD1	1.01±0.25	0.96±0.26	0.95 ±0.19	0.95±0.2	1.09±0.21	1.17±0.26	0.78±0.12*	0.78±0.14
SOD2	0.87±0.46	0.84±0.28	0.89 ±0.31	1±0.24	0.97±0.25	0.96±0.58	0.81±0.21	0.89±0.32
NRF2	0.91±0.53	0.82±0.17	0.74±0.3	0.76±0.18	0.89±0.17	1.33±0.38	0.84±0.28	0.83±0.33
P25								
CAT	0.98±0.41	0.78±0.37	1.09±0.6	1.05±0.24	0.82±0.16	0.97±0.27	0.72±0.13*	0.78±0.16
GSR	0.93±0.31	1±0.15	0.47 ±0.43	0.86±0.12	0.84±0.1	0.96±0.17	0.83±0.14	0.87±0.16
SOD1	1.14±0.17	1.1±0.3	1.05 ±0.04	0.92 ±0.19	0.79±0.15	0.95±0.21	0.74±0.09	0.87±0.23
SOD2	1.12±0.26	1.05±0.35	1.28±0.36	1±0.26	0.78±0.21	0.65±0.41	0.83±0.14	1.02±0.25
NRF2	0.68±0.22	0.93±0.21	0.57±0.56	0.87±0.2	0.74±0.28	0.97±0.18	0.83±0.2	0.81±0.18
E171								
CAT	1.00±0.38	1.15±0.37	1.09±1.27	0.66±0.25	1.01±0.15	1.2±0.28	0.73±0.14*	0.83±0.16
GSR	1.00±0.33	1.08±0.31	0.75±0.09	0.83±0.15	0.98±0.07	1.13±0.12	0.74±0.13*	0.8±0.15*
SOD1	1.18±0.34	1.14±0.47	0.78±0.15	0.72±0.24	0.93±0.18	1.17±0.26	0.85±0.11	0.72±0.12*
SOD2	1.44±0.83	1.07±0.47	0.84±0.22	0.85±0.2	0.87±0.21	0.91±0.67	0.81±0.13	0.83±0.15
NRF2	0.89±0.49	0.87±0.38	0.79±0.27	1.12±0.19	0.85±0.11	1.1±0.37	0.88±0.31	0.96±0.2

[a]Exposure to A12, P25 and E171 for 6 h or 48 h to 50 µg/mL, or for 21 days to 10 or 50 µg/mL affects expression levels for selected oxidative stress regulator genes, as determined by RT-qPCR. Results are expressed as fold-increase above the control (unexposed cells) and expressed as mean ± standard deviation. *$p<0.05$, exposed vs. control, n=3, downregulation is indicated in blue; upregulation is indicated in red.

Table S5. DNA damage caused by TiO_2 particles, assessed with the comet assay[a]

	Caco-2		Caco-2/HT-29-MTX	
	Alkali-labile	+Fpg	Alkali-labile	+Fpg
A12 10 µg/mL 6 h	1.2±0.5	1.0±0.1	0.6±0.1	0.7±0.1
A12 10 µg/mL 48 h	0.7±0.3	1.3±0.1	2±0.9	1.2±0.0
A12 50 µg/mL 6 h	1.1±0.7	1.5 ±0.1	0.9±0.2	0.9±0.1
A12 50 µg/mL 48 h	0.9±0.1	1.1±0.7	2.1±1.5	3.7±1.5
E171 10 µg/mL 6 h	0.5±0.1	1.4±0.3	0.5±0.2	0.9±0.3
E171 10 µg/mL 48 h	0.9±0.1	1.7±0.3	2.6±0.7	1.8±0.9
E171 50 µg/mL 6 h	1.2±0.7	1.2±0.1	0.8±0.1	1.1±0.1
E171 50 µg/mL 48 h	1.5±0.3	1.7±0.1	0.9±0.1	3.5±0.9

[a]Caco-2 and Caco-2/HT29-MTX were exposed to 10 or 50 µg/mL of A12, P25 or E171 for 6 h or 48 h. They were then analyzed using the alkaline version of the comet assay ("alkaline"), or its Fpg-modified version ("+Fpg"). Results are expressed as fold-increase above the control (unexposed cells), as mean ± standard deviation of 3 independent experiments. *P<0.05 vs. control.

Table S6. RT-qPCR analysis of expression levels for endoplasmic reticulum stress markers[a]

	Caco-2				Caco-2/HT29-MTX			
	6 h 50µg/mL	48 h 50µg/mL	21 days 10 µg/mL	21 days 50 µg/mL	6 h 50µg/mL	48 h 50µg/mL	21 days 10 µg/mL	21 days 50 µg/mL
A12								
CHOP	1.16±0.37	0.78±0.09*	0.74± 0.1*	0.8 ±0.17	0.93±0.13	0.8±0.06	0.96±0.17	1.19±0.17*
ATF6	0.94±0.08	0.64±0.17	1.13± 0.23	0.9 ±0.16	0.83±0.2	0.98±0.28	0.8±0.21	1.16±0.37
GRP78	1.08±0.12	1.11±0.17	1.18 ±0.14	0.89 ±0.12	1.17±0.1	0.99±0.14	0.88±0.23	1.01±0.19
IRE-1	0.9±0.16	0.66±0.18	0.9 ±0.18	0.93 ±0.16	0.74±0. 23	0.99±0.21	0.82±0.34	1.23±0.58
sXBP1	0.92±0.08	0.8±0.05	1.08 ±0.12	0.92 ±0.09	0.98±0.07	1.05±0.14	0.93±0.07	1.09±0.34
P25								
CHOP	1±0.25	0.97±0.48	0.75±0.09	0.71±0.12	0.76±0.13	0.96±0.17	1.41±0.6	1.7±0.67*
ATF6	0.98±0.26	0.71±0.21	0.86±0.17	0.6 ±0.12*	0.97±0.21	0.91±0.26	0.94±0.42	1.23±0.31
GRP78	0.95±0.07	0.94±0.14	0.96±0.12	0.72±0.13*	0.96±0.09	1.02±0.06	0.69±0.14*	1.21±0.5
IRE-1	1.22±0.34	0.9±0.34	0.87±0.15	0.79 ±0.19	0.63±0.13	0.72±0.23	1.±0.49	1.38±0.55
sXBP1	0.97±0.07	0.83±0.2	0.85± 0.08	0.77 ±0.12	0.89±0.02	0.99±0.14	0.88±0.14	1.27±0.33
E171								
CHOP	1.08±0.2	0.84±0.17	0.57±0.22*	0.83±0.15	0.93±0.13	0.67±0.06*	0.9±0.03	1.13±0.13
ATF6	0.93±0.2	0.72±0.13*	0.99±0.16	1.11±0.3	0.84±0.2	0.73±0.07*	0.73±0.23	0.84±0.23
GRP78	1.04±0.07	1.01±0.18	1.13±0.13	0.78±0.09*	1.11±0.08	0.91±0.06*	0.79±0.16	1.03±0.16
IRE-1	0.97±0.23	0.67±0.36	1.22±0.21	2.01±0.69	0.65±0.17*	0.71±0.06*	0.58±0.35	0.81±0.31
sXBP1	0.94±0.08	0.92±0.06	1.23±0.37	1.01±0.12	0.93±0.07	0.99±0.1	0.77±0.18	0.87±0.06*

[a]Impact of A12, P25 and E171 exposure (6 h or 48 h to 50 µg/mL; or 21 days to 10 or 50 µg/mL) on expression levels of selected ER stress regulator genes, as determined by RT-qPCR. Results are expressed as fold-increase relative to the control (unexposed cells) and expressed as mean ± standard deviation. *$p<0.05$, exposed vs. control, n=3, downregulation is indicated in blue; upregulation is indicated in red.

References:

Sambuy Y, De Angelis I, Ranaldi G, Scarino ML, Stammati A, Zucco F. 2005. The Caco-2 cell line as a model of the intestinal barrier: influence of cell and culture-related factors on Caco-2 cell functional characteristics. Cell Biol Toxicol 21(1): 1-26.